1. Hassane Ezziane [1], 2. Hamza Houassine[1,2], 3.Samir Moulahoum[1] , 4.Moustafa Sahnoune Chaouche[1]

Research Laboratory of Electrical Engineering and Automatics LREA, University of Medea, Medea, Algeria(1), Department of Electrical Engineering, University of Bouira, Algeria (2)

ORCID. 1. 0000-0002-4875-3226, 2. 0000-0002-1651-6613, 3. 0000-0002-7482-0621, 4. 0000-0002-4331-8604

doi:10.15199/48.2022.01.04

Classifying Transformer Winding Fault Type, Location and Extent using FRA based on Support Vector Machine

Abstract. *In this paper, four common winding faults in power transformers (axial displacement (AD), serial capacitance variation (VSC), ground capacitance variation (VGC), open circuit (OC)) are simulated on a transformer winding model to classify the fault type, location and extent, by applying an intelligent methodology for diagnosing transformer faults, depends on building a comprehensive database by collecting Frequency Responses Analysis (FRA) related to health and faulty conditions and analyzing them using statistical and mathematical indicators, this base that can inventory all possible faults in terms of location and extent, which is used to train a support vector machine (SVM) classifier on the faults included in it, which is then able to classify any new data . The results of the tests showed that the proposed method is characterized by high accuracy in detecting the type of defect, determining its location and the extent of its occurrence, It also contributes to the development of the application of machine learning on transformers.*

Streszczenie.\\ *W tym artykule symulowane są cztery typowe uszkodzenia uzwojeń w transformatorach mocy (przemieszczenie osiowe (AD), szeregowa zmiana pojemności (VSC), zmiana pojemności uziemienia (VGC), obwód otwarty (OC)) na modelu uzwojenia transformatora w celu sklasyfikowania typu zwarcia , lokalizacji i zasięgu, poprzez zastosowanie inteligentnej metodologii diagnozowania uszkodzeń transformatorów, polega na zbudowaniu kompleksowej bazy danych poprzez zbieranie Analizy Odpowiedzi Częstotliwości (FRA) związanej ze stanami zdrowia i wadliwymi oraz analizowanie ich za pomocą wskaźników statystycznych i matematycznych, tej bazy, która może inwentaryzować wszystkie możliwych błędów pod względem lokalizacji i zasięgu, który jest używany do trenowania klasyfikatora maszyny wektora nośnego (SVM) na zawartych w nim błędach, który jest następnie w stanie sklasyfikować dowolne nowe dane. Wyniki badań wykazały, że proponowana metoda charakteryzuje się dużą dokładnością w wykrywaniu rodzaju defektu, określaniu jego lokalizacji oraz zasięgu jej występowania, przyczynia się również do rozwoju zastosowania uczenia maszynowego na transformatorach.* (***Klasyfikacja typu, lokalizacji i zakresu uszkodzenia uzwojenia transformatora za pomocą FRA w oparciu o maszynę wektora nośnego***)

Keywords: Frequency response analysis (FRA),support vector machine (SVM), winding faults,diagnostic.
Słowa kluczowe:. Odpowiedź częstotliwościowa, uszkodzeni uzwojenia

Introduction

Power transformers are one of the most important components of electrical power networks, and as a result of the loss resulting from the sudden breakdown of these transformers, it has become necessary to assess their condition and verify their performance periodically through periodic monitoring strategies. This enables us to shut down the transformer before imminent failure, helping us reduce maintenance costs and save time. But before that, the type, location and extent of the defect must be determined, and this represents a great challenge for researchers.

Many research works have provided techniques for monitoring the state of transformers that depend on temperature measurement [1-4], dissolved gas in oil analysis (DGA) [5-7], Dielectric Response Analysis [8, 9] ,and vibration analysis [10-12], Frequency Response Analysis (FRA) [13-18] which have been widely used due to its accuracy, simplicity, and speed are among the most reliable and sensitive method for evaluating transformer condition as previous researchs shown, where it can determine the defect after comparing the measured frequency response signatures with the transformer health signature.

Therefore, many studies that are concerned with discovering transformer faults have relied on FRA frequency response analysis to diagnose winding defects and determine their location and extent. In the paper [19], the extent of two types of mechanical defects (AD and RD) were estimated using Euclidean distance (ED). and to distinguish between the two defects, Regional ED (RED) and the ratio of maximum ED to minimum RED (MMR) were used. Was applied to the defect simulation results. Either in [20] Three mechanical faults (AD, RD, SDV) detected using the transfer function (TF), Was used Frequency and amplitude weight functions were relied upon to discover the location and extent of the fault, but regarding detecting the types of fault was used the correlation coefficient (CC) for three range.

With the development of artificial intelligence (AI) in recent years, many studies have applied it with the technique of frequency response analysis (FRA) to diagnose faulty transformers, In the paper [21] by transfer function (TF) analysis using Vector fitting (VF), Been trained a probabilistic neural network (PNN) to detecting the type of faults (AD, RD, DSV, SC), But the location and extent have not been determined. Either in the study [22] two features, the TFs measured for four faults (Disc-to-disc, short circuit, RD, and AD) Processing by mathematical indices (IFR, IAR) and VF, They were used to train SVM classifier to detect type and location of Previous faults, The results are compared with ANN, However, the authors did not address the level of faults.

working on a single defect [23] here the authors simulated short circuit fault (low and high-impedance) were applied to the model winding, the support vector regression (SVR) was used to interpret those FRA traces to detect exact fault location, However, the defect level is also not covered in this paper. in [24], The authors apply 4 common faults (DSV, RD, SC, and AD) to the transformer winding, to detect the type, location, and extent of faults by comparing the transfer function (TF) by W-index and used FDA for dimension reduction, The results are satisfactory, but the method is not comprehensive.

Either in [25] the SVM was used with FRA data extracted from a series of experiments were carried out on an actual transformer, and then PSO algorithm is used to optimize SVM model parameters, to be discriminating fault types and degrees of transformer deformation faults .

In general, we noticed that the majority of these studies, especially those that relied on classification algorithms, used non-comprehensive databases, meaning that the observations included in these rules are not sufficient to enumerate all possible cases of fault, and this is because

the fault was tested in some sites and at a certain level only, and therefore if the defect occurred in a new site, the classifier fails to classify it because it was not trained on it, moreover, most of these studies did not address the determination of the level of defects, despite its great importance, therefore, in this paper, We attempted to processing these problems by proposing a methodology based on building a comprehensive database for each fault containing the majority of possible cases in terms of location and extent, with the choosing of an SVM classifier to detect the type, location, and extent of the fault.

2 . Summary of methods employed :

In this paper, we use SVM to predict the type, location and extent of faults, but the most important thing to do that, it's the right choice for the features that are used for training and testing SVM, Therefore we used a mixture of mathematical and statistical indicators (IFR and IAR, ASLE, DABS, IMSE, CC), that will be described here:

2.1 Mathematical indices :

According to previous studies [26],[27], when winding faults occur, the most important transformations observed in FRA frequency responses are peak points and trough (This is shown in Fig .4.a) .

Proceeding from this, we can use the difference in frequency and amplitude as effective indicators for SVM training, the variation of frequency in *i-th* peak and trough points It is indicated by index of frequency ratio (IFR) as follows:

$$IFR_{ti} = \frac{f_{k,ti}}{f_{o,ti}} \quad , \quad IFR_{pi} = \frac{f_{k,pi}}{f_{o,pi}} \tag{1}$$

where ($f_{k,ti}$ and $f_{o,ti}$) and ($f_{k,pi}$ and $f_{o,pi}$) represent the i-th frequency in trough and peak points , respectively

and (k : represents the failure condition , O : is indication of the healthy state) .

with same way we express the variation of amplitude at the *i-th* peak and trough points by index of amplitude ratio (IAR) as follows:

$$IAR_{ti} = \frac{A_{k,ti}}{A_{o,ti}} \quad , \quad IAR_{pi} = \frac{A_{k,pi}}{A_{o,pi}} \tag{2}$$

where ($A_{k,ti}$ and $A_{o,ti}$) and ($A_{k,pi}$ and $A_{o,pi}$) represent the amplitude of impedance at the *i-th* trough and peak points, respectively .

Table .1 Statistical indicators expressions

Indicators	Descriptions
Absolute sum of logarithmic error (ASLE)	$ASLE = \frac{\sum_{i=1}^{N} \lvert 20log_{10}\lvert X_i\rvert - 20log_{10}\lvert Y_i\rvert\rvert}{N}$
Absolute difference (DABS)	$DABS = \frac{\sum_{i=1}^{N} \lvert X_i - Y_i\rvert}{N}$
mean square error (IMSE)	$IMSE = \frac{\sum_{i=1}^{N} (X_i - Y_i)^2}{N}$
correlation coefficient (CC)	$CC(X,Y) = \frac{\sum_{i=1}^{N} (X_i - \bar{X})(Y_i - \bar{Y})}{\sqrt{\sum_{i=1}^{N} (X_i - \bar{X})^2 \sum_{i=1}^{N} (Y_i - \bar{Y})^2}}$

'N' : appear the total size of the data set . 'Xi' and 'Yi' : represents the total of all variables in the data set .'$\bar{X}$ ' and '$\bar{Y}$ ' : represents the mean values of observations.

2.2 Statistical indicators :

With the aim of improving the explanatory ability of FRA We used some statistical parameters that have proven effective such as absolute sum of logarithmic error (ASLE) [28, 29, 31, 32, 34], the absolute difference (DABS) [28, 30, 32, 34], correlation coefficient (CC) [28, 30, 31, 33, 34], mean square error (MSE) [28, 29, 34]. Due to changing of morphological characteristics of FRA signatures in the different frequency bands, We divided the signature into low, medium and high frequency band to improve the reliability of indicators, these indicators apply to all FRA signatures from the set of experiments in Section (3) in the mentioned frequency bands.

Table.1 provides the mathematical expression for the indicators used in this study :

2.3 Support Vector Machine (SVM) :

Support vector machines (SVMs) are powerful yet flexible supervised machine learning algorithms which are used both for classification and regression. But generally, they are used in classification problems, SVM is built upon a solid foundation of statistical learning theory, were proposed by Vapnik [35], nitially it was created to classify into two classes. Then SVM was recently developed as an machine learning algorithm, that's method based on theory of statistical learning theory and the principle of minimum structural risk. It has special advantages to solve The problem of classification of samples is small, and non-linear, And high-dimension,Therefore it is known for its efficiency, specially for classification problems. Which makes it very useful in classification faults in our work [36].

The idea of SVM is simple, It depends on creating a hyperplane or line that separates the data into classes to find the maximum marginal hyperlevel (MMH). The hyperplane is created in an iterative manner to reduce the error [37].

The kernel functions is a mathematical tricks used by SVM algorithms, it's allows is to drop the input data from Low-dimensional to higher dimension space, as for choosing the right function is very important to SVM's performance, among the common kernel functions are mentioned in [38]:

- The linear function :

$$K(x, x') = x.x' \tag{3}$$

- The polynominal kernel function :

$$K(x, x') = (x.x')^d \; or \; (1 + x.x')^d \tag{4}$$

where *d* is the degree of the polynomial.

- Gaussain radial basis functin :

$$K(x, x') = exp\left(-\frac{(x-x')^2}{2\sigma^2}\right) \tag{5}$$

where x and x' denote support vectors and σ is a RBF kernel parameter to be determined.

- Sigmoid kernel function :

$$K(x, x') = tanh(a_0(x.x') + \beta_0) \tag{6}$$

3. Equivalent model of a transformer winding :

In order to apply the proposed methodology, we applied it to a winding of a transformer which was inspected by Ragavan and Satish [39], The equivalent circuit modulation of the transformer winding depends on the FRA frequency response measurement data as follows: a number of sections ($N = 6$), equivalent inductance *(Leq = 6.98mH),* effective capacitance *(Cg, eff = 5.6 ηF, Cg = 0.933 ηF),* resistance Constant current *(Rdc = 8Ω, r = 1.333Ω)* and distribution constant *(α = 7.4833)* , by using the number of sections , the distribution constant and effective capacitance, was calculated value of series capacitance [39], which was found *Cs = 0.6 ηF,* in addition to determine the capacitance Serial from indirect measurement was discussed in [40] by adopting the DPI (zero-gain electrode shape) function described in [41].

Accordingly, the polynomial $P(Cs)$ was determined from estimated the numerical gain factor " $K \approx 1.1275$ " (the value of K was found to be $1 / Ceq$ with Ceq: equivalent input amplitude of the lump pattern [40]), number resonance points $(N = 6)$ The transformative capacitance $(Cg = 0.933\ \eta F)$ such that :

$$P(Cs) = -2.2551Cs6 - 25.8717Cs5 - 37.7484Cs4 - 5.0699Cs3 + 12.3388Cs + 5.5892Cs + 0.662$$

The roots of $P(Cs)$ are: -0.25169 , -0.51095 , -1.20694, -0.32066, -9.79208 and 0.60979 .
Then, the serial capacitance value was determined which is $Cs = 0.60979\ \eta F$. The Table 2 enables us to construct an induction matrix.

Table 2 . Values of Self and Mutual Inductances (*Ls, Mi-j,* in *mH*) [39]

Ls	M1-2	M1-3	M1-4	M1-5	M1-6
0.4310	0.2392	0.1435	0.0947	0.0612	0.0496

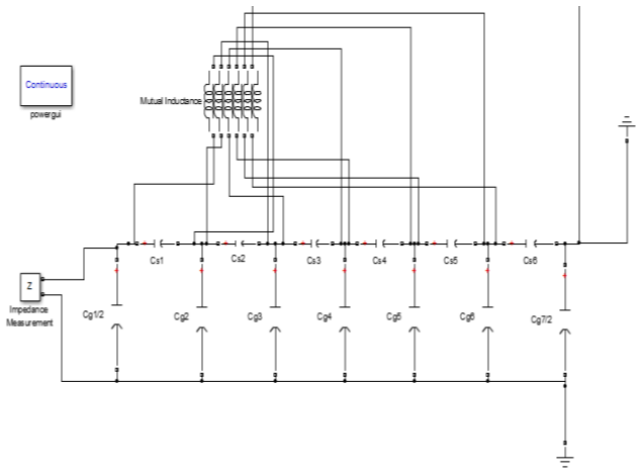

Fig. 1. Six-section synthesized reference circuit [39]

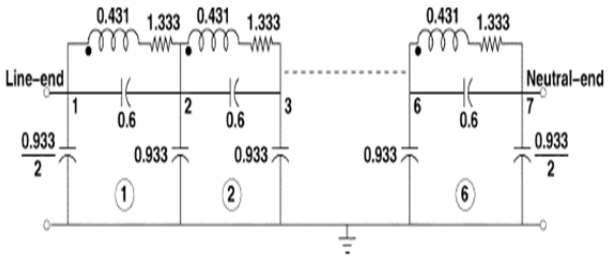

Fig. 2. Detaled model of winding (constructed using MATLAB simulink)

a)

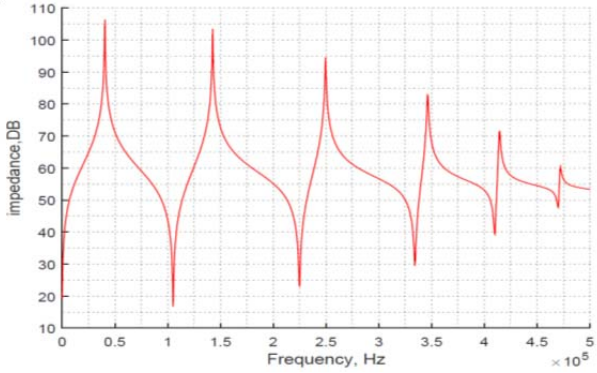

b)

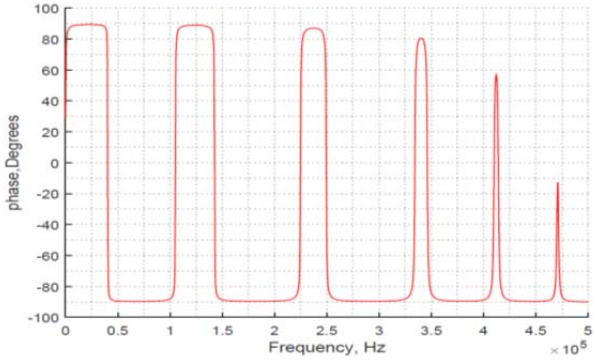

Fig. 3. The frequency response to the healthy status of the model winding . a) Magnitude b) Phase

3.1. Simulation of faults on the winding model :

After validating the model, we use it to study failures cases of winding using the FRA technique. The simulation of faults depends on changing the parameters of the healthy winding model according to the fault to be studied . the defects that have been simulated are as follow:

3.1.1. Fault in the ground capacitance C_g (VGC) :

We can simulate different levels of fault by changing the Cg value (increasing from 10% to 90%) , then we repeat the process on each disk, (Fig. 4.b) shows FRA data in normal and some faulty cases from each disc , and According to (Fig. 4.a) we can see that with increasing fault ratio the resonant frequencies are move to the left regularly .

a)

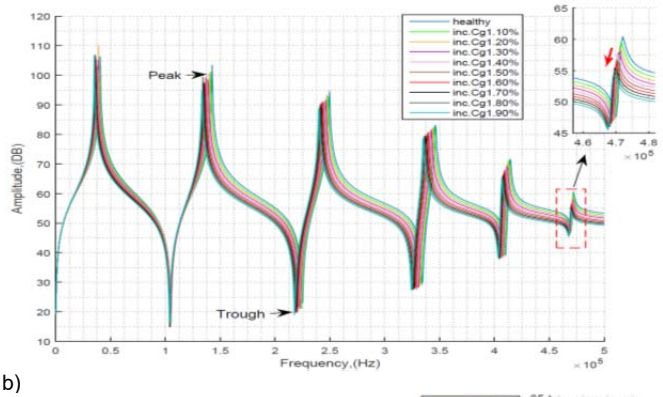

b)

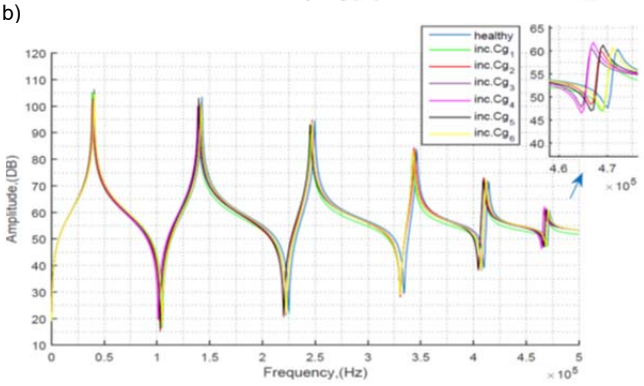

Fig. 4. Frequency response curves of VGC.

3.1.2. Fault in the series capacitance *Cs* (VSC) :

To simulate different levels of this fault , the serial capacity Cs is changed (increasing 10% to 90%) between all disks. Some of the FRA signatures measured between the different disks are shown in (Fig.5.a) , and as presented in (Fig. 5.b) with the fault level increases, the resonant frequencies are moved to the left regularly.

a)

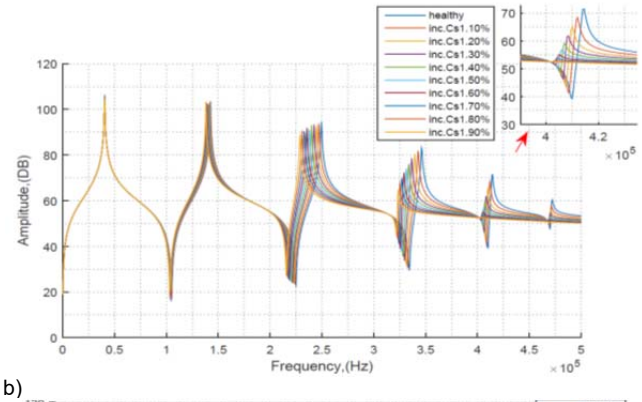

b)

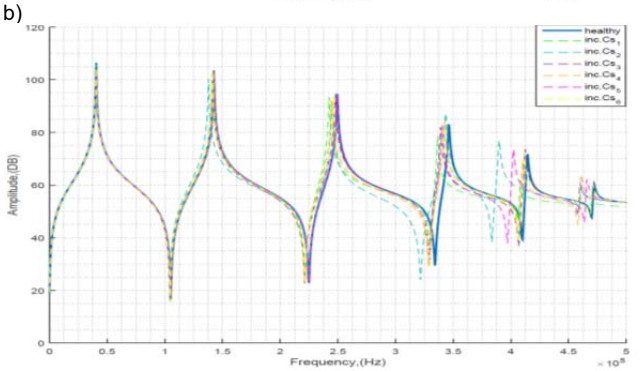

Fig. 5. Frequency response curves of VSC .

3.1.3. Axial displacement fault (AD) :

This defect is the result of unbalanced magnetic forces generated in the upper and lower parts of a certain disk as a result of a short circuit fault [42], we can be simulated this fault by changing the values of the mutual and self inductances of particular discs with the possibility of neglected The capacitance effect [43].

Accordingly, we simulated this type of fault by changing the inductance matrix, for easy visualization, consider the nominal inductance matrix $\mathbb{L}$, corresponding to equation (7), as follows:

(a

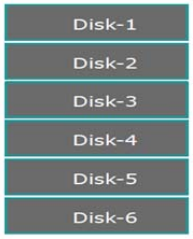

$$\mathbb{L} = \begin{bmatrix} L_{11} & L_{12} & L_{13} & L_{14} & L_{15} & L_{16} \\ L_{12} & L_{22} & L_{23} & L_{24} & L_{25} & L_{26} \\ L_{13} & L_{23} & L_{33} & L_{34} & L_{35} & L_{36} \\ L_{14} & L_{24} & L_{34} & L_{44} & L_{45} & L_{46} \\ L_{15} & L_{25} & L_{35} & L_{45} & L_{55} & L_{56} \\ L_{16} & L_{26} & L_{36} & L_{46} & L_{56} & L_{66} \end{bmatrix}$$

After AD occurs between disks 4 and 5, we notice a change in the inductance matrix, The $\mathbb{L}$ matrix is shown in equation **(8)** and the subject of change (which will be estimated) are highlighted. The rest is unchanged.

(b)

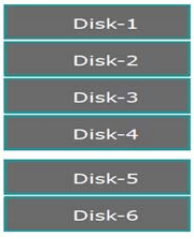

$$\mathbb{L} = \begin{bmatrix} L_{11} & L_{12} & L_{13} & L_{14} & L_{15} & L_{16} \\ L_{12} & L_{22} & L_{23} & L_{24} & L_{25} & L_{26} \\ L_{13} & L_{23} & L_{33} & L_{34} & L_{35} & L_{36} \\ L_{14} & L_{24} & L_{34} & L_{44} & L_{45} & L_{46} \\ L_{15} & L_{25} & L_{35} & L_{45} & L_{55} & L_{56} \\ L_{16} & L_{26} & L_{36} & L_{46} & L_{56} & L_{66} \end{bmatrix}$$

Fig. 6. Schematic of a six disk winding : (a) before and (b) after axial displacement (D4-D5)

We simulated fault in different proportions between each two consecutive disks (D1-D2), (D2-D3), (D3-D4), (D4-D5), (D5-D6) to get different levels of fault , from the (Fig.7.a) we can see the change in the FRA signals starting at 100 kHz , and the change in resonant frequency is related with ratio of displacement, In (Fig.7.b) show the FRA curves resulting from AD simulation among the disks of winding .

a)

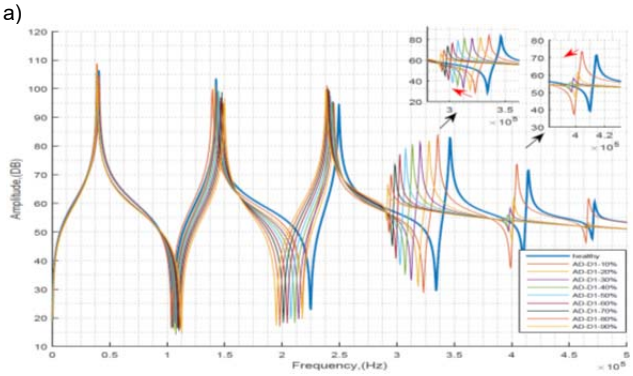

b)b

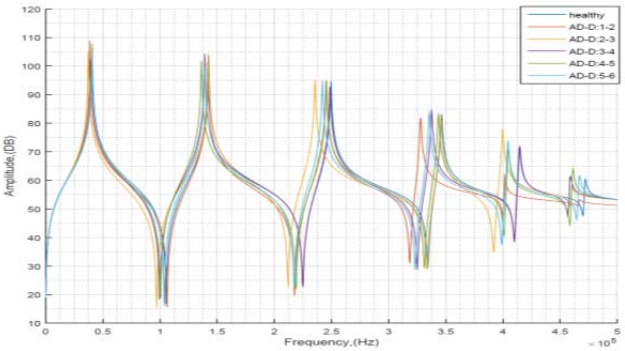

Fig. 7. Frequency response curves of AD

3.1.4. Open circuit fault (OC) :

We simulate this fault by creating an open circuit at all winding disks , the result of simulation fault shown in Fig. 8 is consistent with the results published in [44] , this type of fault can be distinguished from the rest faults easily because it has a significant and clear impact on the FRA signature especially in the low- frequency band.

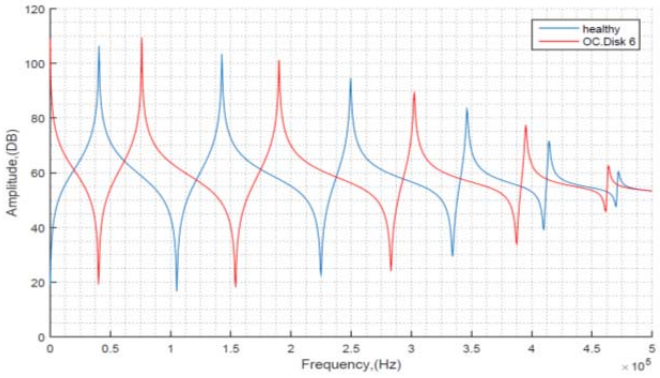

Fig. 8. Frequency response curves of OC

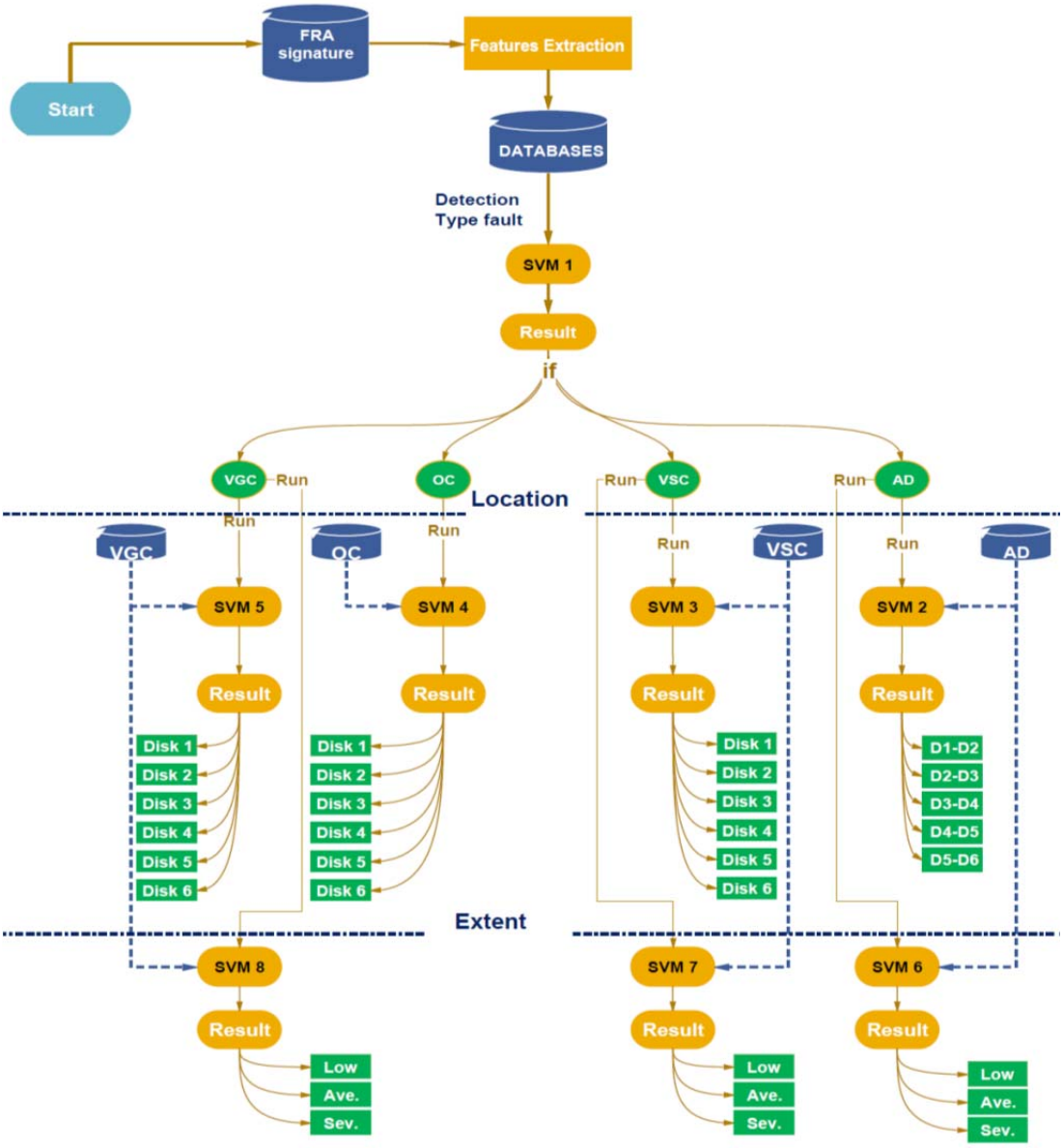

Fig. 9. diagram of proposed methodology

4. Detection methodology applied :

The proposed methodology is based on two key stages: database construction and defect diagnosis. in the first stage, The FRA signatures are collected from simulations of the previous faults. after that, The features are extracted from these signatures using the most appropriate indicators, then a comprehensive database and four sub-bases of the tested faults are constructed by aggregating the obtained features. In the second stage, these bases are used to train and evaluate SVM in order to determine the type, location, and level of faults in the second stage.

The methodology steps can be summarized in the following graph :

After we simulate the four faults 210 times and obtaining the frequency responses, we collect and process these signals using the previously mentioned indicators and extract the features that were used in forming the databases, we will try to explain these steps as follows:

4.1. Feature extraction from FRA signature :

The most important stage is to extract the features, if the specific features summarize the problem accurately then we will get good results, Therefore, it is better to choose indicators with high precise and reliability.

in this study ,The features represent the variance between the reference FRA signal which is the normal condition and the FRAs signals for defective condition. This variance is estimated using mathematical indices such as: IAR and IFR, which can be calculated via Equations (1) - (2) and statistical indicators (ASLE, DABS, IMSE, CC) mentioned in Table 1, these features are used as input for SVM .

4.2. Databases :

From the computed features, five databases are created, They are detailed in the following tables :

4.2.1. Detection fault : In this process we have one database that includes the four faults data we use to detect the type of fault .

Table 3. database (Fault Detection)

N.	Class	Number of observations
1	AD fault	45
2	VSC fault	54 (9 for eash)
3	VGC fault	54
4	OC fault	54

4.2.2 location fault : To discover the location of the defect. Each type needs a special database, so we have formed four databases, the details of which are in the following tables:

Table 4. database for VGC fault (Fault location)

Fault type	Class		Number of observations
Variation C_g fault (VGC)	1	VC_{g1}	54 (9 for eash)
	2	VC_{g2}	
	3	VC_{g3}	
	4	VC_{g4}	
	5	VC_{g5}	
	6	VC_{g6}	

Table 5. database for AD fault (Fault location)

Fault type	class		Number ofobservations
AD fault	1	between 1 - 2 disk	45 (9 for eash)
	2	between 2- 3 disk	
	3	between 3 - 4 disk	
	4	between 4 - 5 disk	
	5	between 5 - 6 disk	

Table 6. database for VSC fault (Fault location)

Fault type	class		Number of observations
Variation Cs fault (VSC)	1	VC_{s1}	54 (9 for eash)
	2	VC_{s2}	
	3	VC_{s3}	
	4	VC_{s4}	
	5	VC_{s5}	
	6	VC_{s6}	

Table 7. database for OC fault (Fault location)

Fault type	class		Number of observations
OC fault	1	Disk 1	54 (9 for eash)
	2	Disk 2	
	3	Disk 3	
	4	Disk 4	
	5	Disk 5	
	6	Disk 6	

4.2.3. Extent fault : to determine the extent of the fault, we use three databases, each database contains one type of faults divided into three classes , Also the previous databases used in the determine location step can be used with only change the output of the SVM :

Table 8. database for VGC or VSC fault (Fault extent)

Typ.	VCg or VCs fault(VGC and VSC)																	
Loc.	D1			D2			D3			D4			D5			D6		
Ext.	Low	Ave.	Sev.	Low	Ave.	Sev.	Low	Ave.	Sev.	Low	Ave.	Sev.	Low	Ave.	Sev.	Low	Ave.	Sev.

Table 9. database for AD fault (Fault extent)

Typ.	AD														
Loc.	D1-D2			D2-D3			D3-D4			D4-D5			D5-D6		
Ext.	Low	Ave.	Sev.	Low	Ave.	Sev.	Low	Ave.	Sev.	Low	Ave.	Sev.	Low	Ave.	Sev.

4.3 Training procedures :

First before training SVM, We need to define the input and output data, For this purpose, we use the set of indicators mentioned in Part Three to train classifier, as Equation (9) represents the input matrix for the complex indicator defined in Equations (1) and (2), which are as follows:

(9)

$$\text{Input}_{\text{Feature1}}=\begin{bmatrix} IFR_{t1,AD_j} & IFR_{t1,VSC_s} & IFR_{t1,VGC_z} & IFR_{t1,OC_l} \\ \vdots & \vdots & \vdots & \vdots \\ IFR_{tk,AD_j} & IFR_{tk,VSC_s} & IFR_{tk,VGC_z} & IFR_{tk,OC_l} \\ IFR_{p1,AD_j} & IFR_{p1,VSC_s} & IFR_{p1,VGC_z} & IFR_{p1,OC_l} \\ \vdots & \vdots & \vdots & \vdots \\ IFR_{pi,AD_j} & IFR_{pi,VSC_s} & IFR_{pi,VGC_z} & IFR_{pi,OC_l} \\ IAR_{t1,AD_j} & IAR_{t1,VSC_s} & IAR_{t1,VGC_z} & IAR_{t1,OC_l} \\ \vdots & \vdots & \vdots & \vdots \\ IAR_{tk,AD_j} & IAR_{tk,VSC_s} & IAR_{tk,VGC_z} & IAR_{tk,OC_l} \\ IAR_{p1,AD_j} & IAR_{p1,VSC_s} & IAR_{p1,VGC_z} & IAR_{p1,OC_l} \\ \vdots & \vdots & \vdots & \vdots \\ IAR_{pi,AD_j} & IAR_{pi,VSC_s} & IAR_{pi,VGC_z} & IAR_{pi,OC_l} \end{bmatrix}$$

where: i , k : show the number of peaks and troughs , respectively in FRA signal .

j , s , z : represent the level of faults AD,VSC and VGC,respectively.

l : indicate the location of OC fault .

As for equations (10) to (13) express the input matrix for the indicators mentioned in Table 1 :

(10) $$\text{Input}_{\text{Feature2}}=\begin{bmatrix} ASLE_{LF,AD_j} & ASLE_{LF,VSC_S} & ASLE_{LF,VGC_Z} & ASLE_{LF,OC_l} \\ ASLE_{MF,AD_j} & ASLE_{MF,VSC_S} & ASLE_{MF,VGC_Z} & ASLE_{MF,OC_l} \\ ASLE_{HF,AD_j} & ASLE_{HF,VSC_S} & ASLE_{HF,VGC_Z} & ASLE_{HF,OC_l} \end{bmatrix}$$

(11) $$\text{Input}_{\text{Feature3}}=\begin{bmatrix} DABS_{LF,AD_j} & DABS_{LF,VSC_S} & DABS_{LF,VGC_Z} & DABS_{LF,OC_l} \\ DABS_{MF,AD_j} & DABS_{MF,VSC_S} & DABS_{MF,VGC_Z} & DABS_{MF,OC_l} \\ DABS_{HF,AD_j} & DABS_{HF,VSC_S} & DABS_{HF,VGC_Z} & DABS_{HF,OC_l} \end{bmatrix}$$

(12) $$\text{Input}_{\text{Feature4}}=\begin{bmatrix} IMSE_{LF,AD_j} & IMSE_{LF,VSC_S} & IMSE_{LF,VGC_Z} & IMSE_{LF,OC_l} \\ IMSE_{MF,AD_j} & IMSE_{MF,VSC_S} & IMSE_{MF,VGC_Z} & IMSE_{MF,OC_l} \\ IMSE_{HF,AD_j} & IMSE_{HF,VSC_S} & IMSE_{HF,VGC_Z} & IMSE_{HF,OC_l} \end{bmatrix}$$

(13) $$\text{Input}_{\text{Feature 5}}=\begin{bmatrix} CC_{LF,AD_j} & CC_{LF,VSC_S} & CC_{LF,VGC_Z} & CC_{LF,OC_l} \\ CC_{MF,AD_j} & CC_{MF,VSC_S} & CC_{MF,VGC_Z} & CC_{MF,OC_l} \\ CC_{HF,AD_j} & CC_{HF,VSC_S} & CC_{HF,VGC_Z} & CC_{HF,OC_l} \end{bmatrix}$$

where :

LF : low-frequency band, MF : Medium frequency band and HF : High frequency band.

SVM output is a one-dimensional vector that indicates the type or location or extent of the fault. After extracting features from FRA signatures extracted from faults and placed in databases, they are used as input for training svm.

In the first step when diagnosing faults types in SVM_1, for the four classes, the input matrix sizes for Features 1 are 22 x 210 and 3 x 210 for Features 2, 3, 4, 5. Next comes the fault locating step, where in SVM_2 for five classes the Input Matrix Sizes for Features 1 are 22 x 45 and 3 x 45 for Features 2, 3, 4, 5 and for SVM_3, SVM_4 and SVM_5 for 6 classes Input matrix sizes for Features 1 It's 22 x 54 and 3 x 54 for features 2, 3, 4, 5.

In the third step, we determined the fault extent for only three fault, as the input matrix sizes for Features 1 were 22 x 54 and 3 x 54 for Features 2, 3, 4, and 5 in SVM_6 for three classes, and for SVM_7 and SVM_8 it was 22 x 54 for Features 1 And 3 x 54 for features 2, 3, 4, 5.
before training any model SVM, the databases were standardized, as an environment for training SVMs, we selected *Libsvm a software package* [45] with the necessary modifications, we adopted the radial basis function (RBF) kernel to train all SVM classifiers, and the optimal values of parameters (C, g) were determined using grid-parameter-search method on the proposed ranges
$log_2\ C$ = *{1, 2,….., 15}* and $log_2\ g$ = {*−15, −14 ,….., 1*}. the accuracy of the trained model is evaluated for each pair of parameters ($log_2\ C$, $log_2\ g$) using the results of five-fold cross-validation on the training data set.
After finding the optimal values for (log_2 C, log_2 g) we train and test the SVM classifier on these values, the whole training and testing procedures are repeated five times with the various training and test partitions of five-fold cross-validation loop was carried out. A procedure using the ***outer–inner–cv*** method, and finally, the rate of test results was computed and reported in the next section.

5 . Classification Results :

5.1 Detection the type of fault : After training, 20% of the data (42 samples) were applied to SVM_1 as a prediction test for fault analysis. In this step, the best test result obtained is displayed on the second line From Table 10, where the table shows that the SVM classifier has succeeded in correctly identifying the type of defects in most cases, it can be seen that all indicators scored 100% for VSC and OC defects, unlike only two indicators (ASLE and IFR. IAR) scored 100% for AD.
The best accuracy rate achieved by the first indicator (IFR. IAR) was 97.61%, as for the other indicators, they also achieved high accuracy that exceeded 90%.
In addition, the diagnostic accuracy rate for 5 training and testing processes appears in the third line of the **Table 10** , which summarizes that the classifier exceeded the threshold of 84% with all indicators, while the first indicator achieved the highest accuracy rate of 92.37%.

Table 10. Classification Result for Type Detection Obtained by SVM method (averaged 5 trials)

Algorithm	classification results			Nb. Samples test	Feature 1 (IFR,IAR)	Feature 2 (ASLE)	Feature 3 (DABS)	Feature 4 (IMSE)	Feature 5 (CC)
Svm 1	Best classification accuracy for a testing set	accuracy of each class on testing set (%)	Class.1(AD)	12	100	100	83.33	91.66	91.66
			Class.2(VSC)	14	100	100	100	100	100
			Class.3(VGC)	10	90	90	90	90	70
			Class.4(OC)	06	100	80	100	100	100
		Accuracy Rate (%)			**97.61**	95.23	92.85	95.23	90.47
	Average classification accuracy for testing sets (%)				**92.37**	87.53	85.94	85.70	84.99

:

5.2 Determine the location of fault
In the second step after detecting the type of fault, We determine the location through one of the four classifiers: SVM_2, SVM_3, SVM_ 4, SVM_ 5. Whereas, for example, if the result of the SVM_1 classifier is Class 1, that is, the AD corruption type, we run SVM_2 for location and SVM_6 for extent.
The same steps that we took previously, we apply it to the four classifiers, so that after training we tested them with 30% of the total samples for each fault.
The best test result for each classifier has been published in the Table 11**.** These results It appears SVM ability to correctly locate faults in most cases, It can be seen that the ASLE and (IFR, IAR) indicators achieved 92.85% accuracy with 100% in four class in SVM _ 2 (AD positioning), as for determining the location of (VSC) , the SVM_3 ranked 94.11% accuracy with four indicators (ASLE, DABS, CC, (IFR, IAR)).
Detecting the location of the third fault OC with SVM_4 was more accurate, reaching 100% in three indicators (ASLE, DABS, (IFR, IAR)), and SVM_5 was also used to locate the fourth fault location (VGC), as only the second index (ASLE) achieved 100% accuracy.
In addition, the table displays the accuracy rate for 5 training and test sets for each of the four databases, where the highest resolution scores shown in bold are indicated using the second ASLE indicator.

Table 11. Classification Results Obtained by SVM method for determine location (averaged 5 trials)

Algorithm	Classification results			Nb. Samples test	Feature 1 (IFR,IAR)	Feature 2 (ASLE)	Feature 3 (DABS)	Feature 4 (IMSE)	Feature 5 (CC)
SVM 2	Best classification accuracy for a testing set (AD fault)	accuracy of each class on testing set (%)	Class.1(D1_D2)	03	100	100	100	66.66	100
			Class.2(D2_D3)	03	100	100	100	100	100
			Class.3(D3_D4)	02	100	100	100	100	100
			Class.4(D4_D5)	04	75	75	75	50	50
			Class.5(D5_D6)	02	100	50	50	50	100
		Accuracy Rate (%)			92.85	**94.85**	85.71	71.42	85.71
	Average classification accuracy for testing sets (%)				88,566	**92,283**	76,424	76,423	80,71

SVM3	Best classification accuracy for a testing set (VSC fault)	accuracy of each class on testing set (%)	Class.1(Disk_1)	03	100	100	100	100	100
			Class.2(Disk_2)	04	75	75	75	50	100
			Class.3(Disk_3)	03	100	100	100	100	100
			Class.4(Disk_4)	02	100	100	100	100	66.66
			Class.5(Disk_5)	03	100	100	100	100	100
			Class.6(Disk_6)	02	100	100	100	50	100
		Accuracy Rate (%)			94.11	**94.11**	94.11	82.35	94.11
	Average classification accuracy for testing sets (%)				86,467	**91,759**	87,643	74,501	88,231
SVM 4	Best classification accuracy for a testing set (OC fault)	accuracy of each class on testing set (%)	Class.1(Disk_1)	04	100	100	100	100	75
			Class.2(Disk_2)	03	100	100	100	66.66	100
			Class.3(Disk_3)	02	100	100	100	100	100
			Class.4(Disk_4)	04	100	100	100	100	100
			Class.5(Disk_5)	02	100	100	100	100	100
			Class.6(Disk_6)	02	100	100	100	100	100
		Accuracy Rate (%)			**100**	**100**	**100**	94.11	94.11
	Average classification accuracy for testing sets (%)				**100**	**100**	**100**	95,288	94,701
SVM 5	Best classification accuracy for a testing set (VGC fault)	accuracy of each class on testing set (%)	Class.1(Disk_1)	03	100	100	100	100	100
			Class.2(Disk_2)	05	80	100	100	100	100
			Class.3(Disk_3)	02	100	100	50	50	50
			Class.4(Disk_4)	02	100	100	100	0	100
			Class.5(Disk_5)	03	100	100	100	100	100
			Class.6(Disk_6)	02	100	100	100	100	100
		Accuracy Rate (%)			94.11	**100**	94.11	76.47	94.11
	Average classification accuracy for testing sets (%)				92,329	**92,347**	88,818	85,289	91,758

5.3 Determine the extent of fault :

As we explained earlier, after detecting the type of fault, we run the SVMs for location and extent together because they use separate databases, at this step we use three classifiers SVM_6-7-8 to determine the extent, The classifiers used 30% of the total samples for testing .

Table 12 shows the best test results and the average accuracy of 5 training and test runs for each data set. Through these results, we can see that although the performance of SVM decreased slightly compared to the two stages of detection the type and location, it was able to distinguish between the three levels with high accuracy.

Moreover, the best classifier results indicated in bold were achieved with feature (2) (ASLE) indicating that the average overall accuracy rate was higher than 81% in the three cases.

Finally, we store the best training for use in diagnosing new samples.

Table.12. Classification Results Obtained by SVM method for determine the extent (averaged 5 trials)

Algorithm	Classification results			Nb. Samples test	Feature1 (IFR ,IAR)	Feature2 (ASLE)	Feature3 (DABS)	Feature4 (IMSE)	Feature5 (CC)
SVM 6	Best classification accuracy for a testing set (AD fault)	accuracy of each class on testing set (%)	Class.1(LOW)	03	66.66	100	100	100	66.66
			Class.2(AVE.)	06	100	83.33	66.66	50	66.66
			Class.3(SEV.)	05	83.33	100	100	100	100
		Accuracy Rate (%)			85.71	**92.85**	85.71	78.57	78.57
	Average classification accuracy for testing sets (%)				77,589	**82,138**	72,852	69,279	68,565
SVM7	Best classification accuracy for a testing set (VSC fault)	accuracy of each class on testing set (%)	Class.1(LOW)	09	100	100	88.88	100	100
			Class.2(AVE.)	04	75	100	100	100	100
			Class.3(SEV.)	04	100	100	80	50	25
		Accuracy Rate (%)			94.11	**100**	88.23	88.23	82.35
	Average classification accuracy for testing sets (%)				78,819	**89,406**	72,347	72,349	81,172
SVM 8	Best classification accuracy for a testing set (VGC fault)	accuracy of each class on testing set (%)	Class.1(LOW)	06	83.33	100	100	66.66	100
			Class.2(AVE.)	05	100	100	80	100	60
			Class.3(SEV.)	06	50	83.33	100	83.33	100
		Accuracy Rate (%)			76.47	**94.11**	94.11	78.57	88.23
	Average classification accuracy for testing sets (%)				65,865	**81,174**	79,996	73,526	78,219

6 . Compaire between Indicators :

In this study, we used several Indicators to explain FRA behavior and the objective is to compare these indicators in the ability to diagnose faults and compatibility with SVM classifie .

for detection type of fault and determining its location, through the previous results, we note that all the features have reached satisfactory results, especially the two features 1 and 2 ((IFA,IAR), ASLE) Which achieve ideal results In this step, in contrast, the results of other features were less accurate than them .

As for determining the extent of the fault, although feature 1 has more training data than others, but some data in feature 1 does not differ with the change of the fault level and thus have similarities between them, For instance, as appeared in Table 13, IFR _t1 in $\mathbf{AD}_{\mathbf{low\ 1}}$ equal to $\mathbf{AD}_{\mathbf{Ave\ 1}}$ and $\mathbf{AD}_{\mathbf{sev\ 1}}$ (Likewise $\mathbf{AD}_{\mathbf{Ave\ 2}}$ equals $\mathbf{AD}_{\mathbf{sev2}}$), In these cases it's hard for the SVM to determine the support vectors, this could lead to an error in estimate the extent of fault .

In feature 2, the difference in data for different levels of fault can be observed (See Table 14). And therefore, It is possible for SVM here to determine the extent of fault with high accuracy. From this, we conclude that the number of training data did not have a significant effect on the accuracy of the classifier.

based on the previous results which show that the classifier with feature 2 produces the best results compared to others feature, thus we can use the ASLE as a reliable indicator to detect the type, and determine location, extent of the transformer winding faults. However, it would be very helpful if some combination Indicators, and therefore can cover the strength of the indicator of weakness of another indicator, for example , feature 1 also achieved good results in detecting and locating the fault with high accuracy but weak in determining the extent.

Therefore, these indicators should be developed with the SVM method for accurate diagnostic of types, location and extent of faults.

Table 13. A set of results for feature 2 (standardized)

Index	**Fault level**							
	$\mathbf{AD}_{\mathbf{low\ 1}}$	$\mathbf{AD}_{\mathbf{low\ 2}}$	$\mathbf{AD}_{\mathbf{Ave.\ 1}}$	$\mathbf{AD}_{\mathbf{Ave.\ 2}}$	$\mathbf{AD}_{\mathbf{Ave.\ 3}}$	$\mathbf{AD}_{\mathbf{Sve.\ 1}}$	$\mathbf{AD}_{\mathbf{Sve.\ 2}}$	$\mathbf{AD}_{\mathbf{Sve.\ 3}}$
$\mathbf{ASLE}_{\mathbf{LF}}$	-0.676012	-0.677798	-0.669369	-0.647780	-0.613772	1.560070	1.854798	2.104687
$\mathbf{ASLE}_{\mathbf{MF}}$	-1.445447	-1.311423	-0.948637	-0.571770	-0.165783	-0.084634	-0.016528	0.113895
$\mathbf{ASLE}_{\mathbf{HF}}$	-0.499308	-0.221592	-0.070255	0.006564	0.025454	0.792141	0.881608	0.930070

Table 14. A set of results for feature 1 (standardized) .

Index	**Fault level**							
	$\mathbf{AD}_{\mathbf{low\ 1}}$	$\mathbf{AD}_{\mathbf{low\ 2}}$	$\mathbf{AD}_{\mathbf{Ave.\ 1}}$	$\mathbf{AD}_{\mathbf{Ave.\ 2}}$	$\mathbf{AD}_{\mathbf{Ave.\ 3}}$	$\mathbf{AD}_{\mathbf{Sve.\ 1}}$	$\mathbf{AD}_{\mathbf{Sve.\ 2}}$	$\mathbf{AD}_{\mathbf{Sve.\ 3}}$
$\mathbf{IFR}_{\mathbf{t1}}$	**-0.910969**	-0.910969	**-0.910969**	**-0.588347**	-0.588347	**-0.910969**	-0.910969	**-0.588347**
$\mathbf{IFR}_{\mathbf{t2}}$	0.060208	0.125784	0.158572	0.224148	0.256936	-0.956219	-1.021795	-1.054583
$\mathbf{IFR}_{\mathbf{p1}}$	-0.741473	-0.950073	-1.119561	-1.276011	-1.406386	-0.337311	-0.337311	-0.337311
$\mathbf{IAR}_{\mathbf{t1}}$	-0.360078	0.724854	-0.887625	-0.000582	0.011679	-1.138633	-0.416323	-0.218432
$\mathbf{IAR}_{\mathbf{t2}}$	-0.598671	-0.807227	-0.773483	-0.759618	-0.902927	0.026536	0.161322	0.138361
$\mathbf{IAR}_{\mathbf{p1}}$	0.640831	0.806196	0.887548	0.919229	-1.701015	1.734438	1.845876	1.947868

Table 15. Classification results obtained for each SVM_s compared with other classifiers results *(averaged 5 trials)*

Detection of :	***Classifier***	***Accuracy rate (%)***
		Featur e 2 (ASLE)
Type	KNN 1	78.15
	RF 1	86.37
	DT 1	81.77
	SVM 1	**88.23**
Location	KNN 2	76.22
	RF 2	80.90
	DT 2	79.17
	SVM 2	**94.28**
	KNN 3	81.60
	RF 3	85.42
	DT 3	82.12
	SVM 3	**91.75**
	KNN 4	**100**
	RF 4	**100**
	DT 4	99.38
	SVM 4	**100**
	KNN 5	78.99
	RF 5	81.94
	DT 5	77.26
	SVM 5	**92.34**
Extent	KNN 6	63.33
	RF 6	80.02
	DT 6	**90.0**
	SVM 6	85.33
	KNN 7	75.72
	RF 7	80.97
	DT 7	75.62
	SVM 7	**89.40**
	KNN 8	74.83
	RF 8	81.59
	DT 8	80.83
	SVM 8	**81.69**

7 . Comparison of Results:

To confirm the ability of the SVM algorithm adopted in the diagnostic methodology proposed in this paper, we applied the methodology with three common classifiers namely Random Forest (RF), k-Nearest Neighbor (kNN), DecisionTree (DT).

These classifiers were applied with databases of the second feature (ASLE) only, which gave the best results in all stages of diagnosis in the previous section. we applied the same cross-validation procedures adopted with SVM, using ***outer–inner–cv*** method, with 5 iterations for each verification process, then calculation Average accuracy rate.

Table 15 displays the classification results for the three methods(KNN, RF, DT) and compares them with previous SVM results,with selected the best classification result for each dataset in bold.

According to the results shown in the table, we notice that the three classifiers gave acceptable results, especially Random Forest (RF), Which had 80.02% minimum average accuracy in all stages of detection. as is common, this classifier provides robust performance whenever the number of training samples is large, As it was with the database for determining the type of defect , but despite its competitive results, However, SVM classifier provided impressive results and proved it's superiority over other methods in all stages of detection: type, location, and the extent, This explains why we have relied on it in the proposed disclosure methodology.

8. Conclusion

In this research, a new methodology was proposed ed to detect type of transformer faults and determine their locations and extent, This methodology based a multi-layer Support Vector Machine (SVM) with the advanced diagnostic technique FRA to determine all locations and extents of faults trained on.

The methodology was verified by building a comprehensive database that contains four common faults of the transformer winding model at different locations and levels , then, using the SVM on three steps, we were able to diagnose the types of faults and determine their location and extent with high accuracy.

The data relates to five features and the aim is to determine the best feature that can deal with the classification algorithm while using the standardization technique to increase accuracy, the results showed through the verification process that the SVM based method using feature 2 (ASLE indicator) can distinguish accurately between types of faults : AD, VGC, VSC , OC and to detect their location and extent, maintaining the best training essential to classify any new data not included in the primary database.

According to the previous results, the method has proven its ability and is able to make a good addition to the development of machine learning in transformers, but with that, if a new type of fault appears, i.e. not included in the database, the classification algorithm fails to diagnose it, Therefore, further work is planned regarding the detection of unknown faults.

Authors:
Mr. Ezziane Hassane, Ph.D. student, Laboratory of Electrical Engineering and Automatics LREA, Department of Electrical Engineering, University of Yahia Fares, Medea, Algeria,
E-mail: ezziane.hassan2051@gmail.com
Dr. Hamza Houassine, Laboratory of Electrical Engineering and Automatics LREA, Department of Electrical Engineering, University of Bouira, Algeria, E-mail:hamza_houassine@yahoo.fr
prof. Samir Moulahoum, Laboratory of Electrical Engineering and Automatics LREA, Department of Electrical Engineering, University of Yahia Fares, Medea, Algeria,
E-mail:samir.moulahoum@gmail.com
Dr. Moustafa Sahnoune Chaouche, Laboratory of Electrical Engineering and Automatics LREA, Department of Electrical Engineering, University of Yahia Fares, Medea, Algeria,
E-mail: moustafa-chaouche@hotmail.fr

REFERENCES

[1] Samimi, M.H., Tenbohlen, S.: 'Using the temperature dependency of the FRA to evaluate the pressure of the transformer press ring', IEEE Trans. Power Deliv., 2018, 33, (4), pp. 2050–2052
[2] Abbasi, A., Seifi, A.: 'Fast and perfect damping circuit for ferroresonance phenomena in coupling capacitor voltage transformers', Electr. Power Compon. Syst., 2009, 37, (4), pp. 393–402
[3] Bagheri, M., Phung, B., Blackburn, T.: 'Influence of temperature and moisture content on frequency response analysis of transformer winding', IEEE Trans. Dielectr. Electr. Insul., 2014, 21, (3), pp. 1393–1404
[4] Mariprasath, T., Kirubakaran, V.: 'A real time study on condition monitoring of distribution transformer using thermal imager', Infrared Phys. Technol., 2018, 90, pp. 78–86
[5] Roncero-Clemente, C., Roanes-Lozano, E. 'A multi-criteria computer package for power transformer fault detection and diagnosis', Appl. Math. Comput., 2017, 319, pp. 153–1642
[6] Abu -Siada, A., Islam, S.: 'A new approach to identify power transformer criticality and asset management decision based on dissolved gas-in-oil analysis', IEEE Trans Dielectr. Electr. Insul., 2012, 19, (3), pp. 1007–1012
[7] Huang, Y.C., Sun, H.C.: 'Dissolved gas analysis of mineral oil for power transformer fault diagnosis using fuzzy logic', IEEE Trans. Dielectrics Electr. Insul., 2013, 20, (3), pp. 974–981
[8] Blennow, J., Ekanayake, C., Walczak, K., et al.: 'Field experiences with measurements of dielectric response in frequency domain for power transformer diagnostics', IEEE Trans. Power Deliv., 2006, 21, (2), pp. 681– 688
[9] Gubansky, S.M., Boss, P., Csépes, G., et al.: 'Dielectric response methods for diagnostics of power transformers', IEEE Electr. Insul. Mag., 2003, 19, (2), pp. 12–18
[10] Zheng, J., Pan, J., Huang, H.: 'An experimental study of winding vibration of a single-phase power transformer using a laser Doppler vibrometer', Appl. Acoust., 2015, 87, pp. 30–37
[11] Zhou, H., Hong, K., Huang, H., et al.: 'Transformer winding fault detection by vibration analysis methods', Appl. Acoust., 2016, 114, pp. 136–146
[12] Wang, Y., Pan, J.: 'Comparison of mechanically and electrically excited vibration frequency responses of a small distribution transformer', IEEE Trans. Power Deliv., 2017, 32, (3), pp. 1173–1180
[13] Hashemnia, N., Abu-Siada, A., & Islam, S. (2013). *Impact of axial displacement on power transformer FRA signature. IEEE Power & Energy Society General Meeting.* doi:10.1109/pesmg.2013.6672949 .
[14] Pleite, J., Gonzalez, C., Vazquez, J., & Lazaro, A. (n.d.).(2006). Power Transfomer Core Fault Diagnosis Using Frequency Response Analysis. MELECON 2006 - 2006 IEEE Mediterranean Electrotechnical Conference. doi:10.1109/melcon.2006.1653298
[15] Rahimpour, E., Christian, J., Feser, K., & Mohseni, H. (2003). Transfer function method to diagnose axial displacement and radial deformation of transformer windings. IEEE Transactions on Power Delivery, 18(2), 493–505. doi:10.1109/tpwrd.2003.809692
[16] Ryder, S. A. (n.d.).(2002). Transformer diagnosis using frequency response analysis: results from fault simulations. IEEE Power Engineering Society Summer Meeting,. doi:10.1109/pess.2002.1043265 .
[17] Bagheri, M., Naderi, M.S., Blackburn, T.R.(2012). A case study on FRA capability in detection of mechanical defects within a 400 MVA transformer. CIGRE, Paris, France, pp. 1–9 .
[18] Behjat, V., Vahedi, A., Setayeshmehr, A., Borsi, H., & Gockenbach, E. (2011). *Diagnosing Shorted Turns on the Windings of Power Transformers Based Upon Online FRA Using Capacitive and Inductive Couplings. IEEE Transactions*

on Power Delivery, 26(4), 2123–2133. doi:10.1109/tpwrd.2011.2151285 .
[19] Pourhossein, K., Gharehpetian, G. B., Rahimpour, E., & Araabi, B. N. (2012). *A probabilistic feature to determine type and extent of winding mechanical defects in power transformers. Electric Power Systems Research, 82(1), 1–10.* doi:10.1016/j.epsr.2011.08.010 .
[20] Rahimpour, E., Jabbari, M., & Tenbohlen, S. (2010). *Mathematical Comparison Methods to Assess Transfer Functions of Transformers to Detect Different Types of Mechanical Faults. IEEE Transactions on Power Delivery, 25(4), 2544–2555.* doi:10.1109/tpwrd.2010.2054840 .
[21] Bigdeli, M., Vakilian, M., & Rahimpour, E. (2011). *A probabilistic neural network classifier-based method for transformer winding fault identification through its transfer function measurement. International Transactions on Electrical Energy Systems, 23(3), 392–404.* doi:10.1002/etep.668 .
[22] Bigdeli, M., Vakilian, M., & Rahimpour, E. (2012). *Transformer winding faults classification based on transfer function analysis by support vector machine. IET Electric Power Applications, 6(5), 268.* doi:10.1049/iet-epa.2011.0232 .
[23] Moradzadeh, A., & Pourhossein, K. (2019). Application of Support Vector Machines to Locate Minor Short Circuits in Transformer Windings. 2019 54th International Universities Power Engineering Conference (UPEC). doi:10.1109/upec.2019.8893542 .
[24] Tarimoradi, H., & Gharehpetian, G. B. (2017). Novel Calculation Method of Indices to Improve Classification of Transformer Winding Fault Type, Location, and Extent. IEEE Transactions on Industrial Informatics, 13(4), 1531–1540. doi:10.1109/tii.2017.2651954 .
[25] J. Liu, Z. Zhao, C. Tang, C. Yao, C. Li and S. Islam, "Classifying Transformer Winding Deformation Fault Types and Degrees Using FRA Based on Support Vector Machine," in IEEE Access, vol. 7, pp. 112494-112504, 2019, doi: 10.1109/ACCESS.2019.2932497.
[26] [Rahimpour, E., Christian, J., Feser, K., & Mohseni, H. (2003). *Transfer function method to diagnose axial displacement and radial deformation of transformer windings. IEEE Transactions on Power Delivery, 18(2), 493–505.* doi:10.1109/tpwrd.2003.809692.
[27] Ragavan, K., & Satish, L. (2008). *Construction of Physically Realizable Driving-Point Function From Measured Frequency Response Data on a Model Winding. IEEE Transactions on Power Delivery, 23(2), 760–767.* doi:10.1109/tpwrd.2008.915815 .
[28] Behjat, V., & Mahvi, M. (2015). *Statistical approach for interpretation of power transformers frequency response analysis results. IET Science, Measurement & Technology, 9(3), 367–375.* doi:10.1049/iet-smt.2014.0097 .
[29] [Kim, J.-W., Park, B., Jeong, S. C., Kim, S. W., & Park, P. (2005). *Fault Diagnosis of a Power Transformer Using an Improved Frequency-Response Analysis. IEEE Transactions on Power Delivery, 20(1), 169–178.* doi:10.1109/tpwrd.2004.835428 .
[30] Secue, J., & Mombello, E. (2008). *New methodology for diagnosing faults in power transformer windings through the Sweep Frequency Response Analysis (SFRA). 2008 IEEE/PES Transmission and Distribution Conference and Exposition: Latin America.* doi:10.1109/tdc-la.2008.4641689 .
[31] Nirgude, P.M., Ashokraju, D., Rajkumar, A.D., and al.(2008). Application of numerical evaluation techniques for interpreting frequency response measurements in power transformers, IET Sci. Meas. Technol., 2008, 2, (5), pp. 275–285 .doi: 10.1049/iet-smt:20070072 .
[32] Secue, J. R., & Mombello, E. (2008). Sweep frequency response analysis (SFRA) for the assessment of winding displacements and deformation in power transformers. Electric Power Systems Research, 78(6), 1119–1128. doi:10.1016/j.epsr.2007.08.005 .
[33] Xu, D.K., Fu, C.Z., Li, Y.M. (1999) .Application of artificial neural network to the detection of the transformer winding deformation. Presented at 11th Int. Symp. on High Voltage Engineering (Conf. Publ. No. 467), London, UK,vol. 5, pp. 220–223. doi: 10.1049/cp:19990925
[34] Badgujar, K.P., Maoyafikuddin, M., Kulkarni, S.V.(2012).Alternative statistical techniques for aiding SFRA diagnostics in transformers, IET Gener. Transm. Distrib., 2012, 6, (3), pp. 189–198 .doi: 10.1049/iet-gtd.2011.0268 .
[35] Vapnik, V.(1995).The nature of statistical learning theory (Springer Verlag, New York).
[36] Zhao, Z., Tang, C., Zhou, Q., Xu, L., Gui, Y., & Yao, C. (2017). *Identification of Power Transformer Winding Mechanical Fault Types Based on Online IFRA by Support Vector Machine. Energies, 10(12), 2022.* doi:10.3390/en10122022 .
[37] Avinash , Navlani . SUPPORT VECTOR MACHINES WITH SCIKIT-LEARN . *datacamp*, **27.Dec.2019,** https://www.datacamp.com/community/tutorials/svm-classification-scikit-learn-python . accessed on Jul. 25, 2020.
[38] Bacha, K., Souahlia, S., & Gossa, M. (2012). *Power transformer fault diagnosis based on dissolved gas analysis by support vector machine. Electric Power Systems Research, 83(1), 73–79.* doi:10.1016/j.epsr.2011.09.012 .
[39] Ragavan, K., & Satish, L. (2007). *Localization of Changes in a Model Winding Based on Terminal Measurements: Experimental Study. IEEE Transactions on Power Delivery, 22(3), 1557–1565.* doi:10.1109/tpwrd.2006.886789 .
[40] Pramanik, S., & Satish, L. (2011). *Estimation of Series Capacitance of a Transformer Winding Based on Frequency-Response Data: An Indirect Measurement Approach. IEEE Transactions on Power Delivery, 26(4), 2870–2878.* doi:10.1109/tpwrd.2011.2167247
[41] Ragavan, K., & Satish, L. (2008). *Construction of Physically Realizable Driving-Point Function From Measured Frequency Response Data on a Model Winding. IEEE Transactions on Power Delivery, 23(2), 760–767.* doi:10.1109/tpwrd.2008.915815
[42] Hashemnia, N., Abu-Siada, A., Masoum, M. A. S., & Islam, S. M. (2012). *Characterization of transformer FRA signature under various winding faults. 2012 IEEE International Conference on Condition Monitoring and Diagnosis.* doi:10.1109/cmd.2012.6416174
[43] Abu-Siada, A., & Islam, S. (2012). *A Novel Online Technique to Detect Power Transformer Winding Faults. IEEE Transactions on Power Delivery, 27(2), 849–857.* doi:10.1109/tpwrd.2011.2180932
[44] Pandya, A. A., & Parekh, B. R. (2014). *Interpretation of Sweep Frequency Response Analysis (SFRA) traces for the open circuit and short circuit winding fault damages of the power transformer. International Journal of Electrical Power & Energy Systems, 62, 890–896.* doi:10.1016/j.ijepes.2014.05.011 .
[45] https://www.csie.ntu.edu.tw/~cjlin/libsvm/